

*Work supported by the U. S. Atomic Energy Commission.

¹B. Hamermesh, J. E. Monahan, and R. K. Smither, *Ann. Phys. (N.Y.)* **13**, 307 (1961).

²O. A. Wasson, R. E. Chrien, M. R. Bhat, M. A. Lone, and M. Beer, *Phys. Rev.* **173**, 1170 (1968).

³T. von Egidy, E. Bieber, and T. W. Elze, *Z. Physik* **195**, 489 (1966).

⁴R. L. Auble, *Nucl. Data B6*(No. 4), 319 (1971).

⁵M. Bonitz, *Nucl. Phys.* **A118**, 478 (1968).

⁶K. E. G. Löbner, J. Klockner, H. Schimmer, and P. Kienle, *Z. Physik* **235**, 254 (1970).

⁷R. Van Lieshout, R. K. Girgis, R. A. Ricci, and A. H.

Wapstra, *Nucl. Phys.* **25**, 703 (1962).

⁸Y. W. Chan, W. B. Ewbank, W. A. Nierenberg, and H. A. Shugart, *Phys. Rev.* **127**, 572 (1962).

⁹A. H. Wapstra, P. F. A. Goudsmit, J. F. W. Jansen, J. Konijn, K. E. G. Löbner, G. J. Nijgh, and S. A. de Wit, *Nucl. Phys.* **A93**, 527 (1967).

¹⁰F. Bacon, G. Kaindl, H. E. Mahnke, and D. A. Shirley, *Phys. Letters* **37B**, 181 (1971).

¹¹K. Sakai and P. J. Daly, *Nucl. Phys.* **A118**, 361 (1968).

¹²F. Bacon, G. Kaindl, H. E. Mahnke, and D. A. Shirley, *Bull. Am. Phys. Soc.* **17**, 658 (1972).

¹³B. Rosner, J. Felsteiner, H. Lindeman, and D. Zeller-mayer, *Nucl. Phys.* **A172**, 643 (1971).

Levels of $^{155, 157, 159, 161}\text{Tb}$ Excited in Helium-Induced Single-Proton-Transfer Reactions*

J. S. Boyno† and J. R. Huizenga

*Nuclear Structure Research Laboratory and Departments of Chemistry and Physics,
University of Rochester, Rochester, New York 14627*

(Received 17 July 1972)

Energy levels of $^{155, 157, 159, 161}\text{Tb}$ have been studied through the ($^3\text{He}, d$) and (α, t) reactions on $^{154, 156, 158, 160}\text{Gd}$, run with 25.5-MeV ^3He and 27.0-MeV α particles, respectively. Distorted-wave Born-approximation analysis was used to interpret the reaction results, with transferred l values obtained from the comparison of the experimental and theoretical values of the cross-section ratio, $R = d\sigma(^3\text{He}, d)/d\sigma(\alpha, t)$. The spectroscopic information obtained was compared to the theoretical predictions of the Nilsson model. Corrective terms added included the Coriolis and pairing interactions. Many of the levels excited were identified as members of rotational bands built on Nilsson single-particle configurations. Identified in all four nuclei are the [411 \dagger], [413 \dagger], [532 \dagger], [404 \dagger], [402 \dagger], and [411 \dagger] Nilsson configurations. Other bands identified are the [541 \dagger] in $^{157, 159, 161}\text{Tb}$, the [523 \dagger] in $^{159, 161}\text{Tb}$, the [411 \dagger] γ mixed configuration in $^{155, 157, 159}\text{Tb}$, and the [514 \dagger] configuration in ^{155}Tb .

I. INTRODUCTION

Single-nucleon-transfer reactions have proved to be a sensitive means of probing nuclear structure. These reactions ordinarily complement nuclear structure studies performed by following radioactive decay, or by inducing Coulomb excitation.

Satchler¹ has pointed out the usefulness of these reactions in the study of deformed nuclei, where the splitting of strength among the members of a rotational band is dependent on the structure of the intrinsic state. This makes the single-nucleon-transfer reaction suitable for the identification of configurations whose structure is approximated by the Nilsson model.

Proton-transfer reactions on deformed nuclei are few in number, due in large part to the experimental difficulties inherent in a (d, n) reaction and to the previous lack of suitable beams of ^3He , ^4He , or heavier ions. Recently with the advent of

higher-energy accelerators, high-resolution spectrographs, and sizable beams of negative He ions, He-induced proton-transfer reactions have become experimentally feasible, even in the actinide region.²

This paper is concerned with an investigation of the levels of $^{155, 157, 159, 161}\text{Tb}$ by ($^3\text{He}, d$) and (α, t) reactions. The stable Gd targets used for these proton-transfer reactions start at the edge of the deformed region, $N=90$. We studied Tb nuclei with neutron numbers $N=90, 92, 94, 96$, which gave us the opportunity to observe the levels occupied by the 65th proton as deformation changed quickly.

The (α, t) reaction, by virtue of the fact that it involves breakup of the α particle favors higher momentum transfer than the ($^3\text{He}, d$) reaction. The ratio $R = d\sigma(^3\text{He}, d)/d\sigma(\alpha, t)$ is a sensitive measure of the momentum transfer so that l values are obtained without the use of angular distributions.

The low-lying levels of these nuclei have been

investigated through various other means, as detailed in the excellent review of Bunker and Reich.³ The addition of our charged-particle reaction data to the previously known level schemes has enabled us to provide a more complete description of these nuclei. Systematic trends can be interpreted as the effects of changing deformation on the single-particle energies and intensities predicted by the theoretical model.

II. EXPERIMENTAL PROCEDURE AND RESULTS

This experimental work was performed with the University of Rochester tandem Van de Graaff accelerator. For the $(^3\text{He}, d)$ runs, a beam of 25.5-MeV ^3He particles was used to bombard thin targets of nearly isotopically⁴ pure $^{154,156,158,160}\text{Gd}$. The lab angle for the $^{154}\text{Gd}(^3\text{He}, d)$ exposure was $\theta_{\text{lab}} = 80^\circ$, while the other $(^3\text{He}, d)$ experiments were run at 60° . The angle chosen in each case was an angle where the emulsion plate was free of any substantial impurity. The emergent deuterons were analyzed in an Enge-type magnetic spectrograph, and recorded on Kodak NTB 50- μm nuclear emulsion plates which were covered with thin aluminum absorbers which intensified the deuteron tracks.

The same targets were used for the (α, t) runs, where a beam of 27.0-MeV α particles was employed. The experiments were run at a lab angle of 60° , and the $^{156,158,160}\text{Gd}(\alpha, t)$ experiments were performed at $\theta_{\text{lab}} = 90^\circ$ as well. The emergent tritons were analyzed in the same manner as the deuterons, although an absorber only 25 μm thick was used, since the tritons are at the optimum energy for track density when they leave the nucleus.

In every experiment the elastic pulses were monitored in the scattering chamber, and a sep-

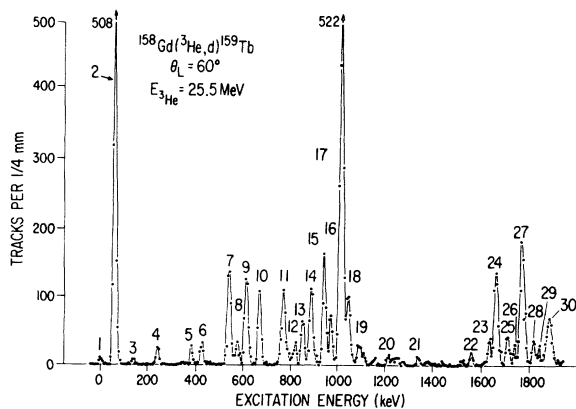


FIG. 1. Spectrum recorded from the $^{158}\text{Gd}(^3\text{He}, d)^{159}\text{Tb}$ reaction at $\theta_{\text{lab}} = 60^\circ$.

arate experimental determination of the elastic scattering cross section allowed us to obtain absolute differential cross sections for the transfer reactions.

A typical $(^3\text{He}, d)$ spectrum is shown in Fig. 1, and an (α, t) experiment leading to the same levels in Fig. 2. Experimental resolution averaged better than 20 keV full width at half maximum. Absolute excitation energies were obtained by identification of the ground-state band in each experiment. The $I=K$ member of this band was set to 0 keV excitation in each case.

The absolute differential cross sections and excitation energies obtained for the excited states of the various nuclei are given in Tables I-IV, along with the results of the analysis, which is discussed in the next section.

III. THEORETICAL ANALYSIS

The differential cross section for the transfer of a single particle in stripping to a deformed odd- A final nucleus may be written

$$\left(\frac{d\sigma}{d\Omega}\right)_{0^+ \rightarrow I=J} = 2C_{JI}^2 U^2 N\sigma_{TDW}, \quad (1)$$

where $N\sigma_{TDW}$ is the renormalized distorted-wave Born-approximation (DWBA) cross section for the transfer of a particle with angular momentum l . The U^2 is an emptiness probability of the state under consideration, calculated by estimating the pairing effects. The C_{JI} are the expansion coefficients of a particular Nilsson state when it is written in terms of spherical eigenfunctions:

$$|NK\rangle = \sum_{j_1} C_{j_1} |Nl j_1 m\rangle. \quad (2)$$

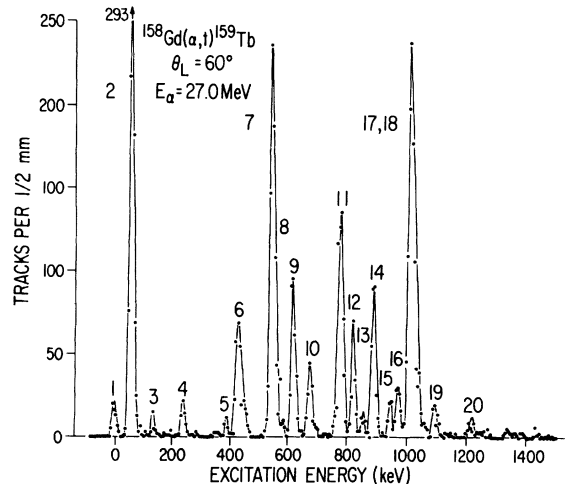


FIG. 2. Spectrum recorded from the $^{158}\text{Gd}(\alpha, t)^{159}\text{Tb}$ reaction at $\theta_{\text{lab}} = 60^\circ$. The individual peak numbers correspond to those in Fig. 1.

TABLE I. ^{155}Tb spectroscopic information. Assignments in parentheses are uncertain; in double parentheses, very uncertain.

Line	$E \pm \Delta E$	$\left(\frac{d\sigma}{d\Omega}\right)_{(\alpha, d)}$ ($\mu\text{b}/\text{sr}$) 80°	$\left(\frac{d\sigma}{d\Omega}\right)_{(\alpha, t)}$ ($\mu\text{b}/\text{sr}$) 60°	Assignment	$S_{\text{EXP}}^{\text{AV}}$	S_{TH}	S_{MIX}	U^2
1	0 ± 4	1.2 ± 0.3	2.0 ± 0.4	$\frac{3}{2}^+$ [411†]	0.05	0.02	0.01	0.6
2	64 ± 2	34.9 ± 2.8	48.6 ± 3.2	$\frac{5}{2}^+$ [411†]	1.2	1.0	1.4	0.6
3	152 ± 3	2.5 ± 0.6	3.4 ± 0.4	$\frac{7}{2}^+$ [411†]	0.20	0.13	0.28	0.6
4	249 ± 5	2.8 ± 0.7		$\frac{7}{2}^-$ [532†]	0.06 ^a	0.02	0.03	0.4
5	275 ± 4	6.1 ± 1.0	{3.8 ± 0.3}	$\frac{3}{2}^+$ [411†], $\frac{5}{2}^+$ [413†]	0.14 ^a , 0.08 ^a	0.04, 0.02	0.04, 0.05	0.6, 0.4
6	332 ± 2	12.8 ± 1.5	31.1 ± 2.2	$\frac{7}{2}^+$ [413†]	1.3	0.76	2.1	0.4
7	395 ± 3	21.3 ± 1.5	76.7 ± 2.3	$\frac{11}{2}^-$ [532†]	2.6	0.96	3.4	0.4
8	424 ± 6	2.5 ± 0.7						
9	456 ± 2	5.0 ± 0.7	17.1 ± 0.9	($\frac{7}{2}^+$ [404†])	0.48	1.6	0.10	0.8
10	494 ± 3	50.4 ± 7.5	46.5 ± 1.9	($\frac{5}{2}^+$ [402†])	1.6	1.7	1.2	0.9
11	559 ± 3	10.2 ± 3.6	22.1 ± 0.5					
12	612 ± 3	7.9 ± 1.0	6.1 ± 0.4					
13	670 ± 5	2.4 ± 0.5						
14	722 ± 4	6.3 ± 1.8	3.2 ± 0.6					
15	750 ± 3	13.7 ± 2.1	7.1 ± 2.2	($\frac{1}{2}^+$, $\frac{3}{2}^+$ [411†])	0.06, 0.26 ^a	0.23, 1.1	0.23, 1.1	0.9
16	768 ± 10		2.0 ± 1.7	(($\frac{1}{2}^+$ [411†]γ))	0.10			
17	802 ± 3	4.0 ± 1.2	2.2 ± 0.7	(($\frac{3}{2}^+$ [411†]γ))	0.10			
18	829 ± 3	7.9 ± 1.1	10.3 ± 1.0					
19	859 ± 3	16.4 ± 4.0	7.6 ± 0.8	(($\frac{5}{2}^+$ [411†]γ))	0.35			
20	900 ± 5	8.6 ± 1.2	5.4 ± 0.6					
21	936 ± 3	11.4 ± 1.4	4.4 ± 0.6	($\frac{3}{2}^+$ [411†])	0.27	0.30	0.21	0.9
22	963 ± 6	4.4 ± 0.7	1.1 ± 0.6					
23	1032 ± 3	3.8 ± 0.7	9.0 ± 0.7	($\frac{11}{2}^-$ [514†])	0.46	2.0	1.0	1.0
24	1061 ± 3	2.5 ± 0.7	7.6 ± 1.5					
25	1087 ± 5	10.1 ± 0.9	7.0 ± 4.6					
26	1112 ± 4	31.6 ± 1.6	4.5 ± 4.5					
27	1131 ± 5		2.4 ± 0.8					
28	1205 ± 5	2.6 ± 0.9						
29	1229 ± 10	1.5 ± 0.9						
30	1260 ± 5	6.2 ± 1.0						
31	1314 ± 4	2.4 ± 0.6						
32	1354 ± 3	4.6 ± 0.7						
33	1446 ± 6	1.1 ± 0.5						
34	1471 ± 10	5.2 ± 5.2						

^a Peak believed to be a multiplet; S extracted by dividing experimental strength in ratio of theoretical strengths.

The quantity σ_{IDW} was calculated with the DWBA code DWUCK. The optical-model parameters used were those obtained from work in the lead region⁵⁻⁷ which have been found to adequately describe proton-transfer work in the rare-earth region.⁸ These parameters are given in Table V. Spin-orbit effects were not included, since the addition of a spin-orbit term similar to that used in Ref. 8 was found to have a small effect on the magnitude of the cross sections. Finite-range effects were similarly neglected, and the inner radial cutoff was

set to zero in all cases. The renormalization constants N were adjusted using experimental data and shall be discussed separately. Theoretical estimates of the spectroscopic factor $S = 2C_{ji}^2 U^2$ were obtained by modifying the results of the Nilsson calculation to include the pairing effects.

Nilsson levels were calculated using the expanded form of the Nilsson Hamiltonian⁹ which includes hexadecapole deformation. The ϵ_4 term used was $\epsilon_4 = -0.04$, as given in Ref. 9. All mass-dependent parameters were adjusted to $A = 159$. Changing A

TABLE II. ¹⁵⁷Tb spectroscopic information. Assignments in parentheses are uncertain.

Line	$E \pm \Delta E$	$\left(\frac{d\sigma}{d\Omega}\right)_{\beta_{He,d}}$ ($\mu\text{b}/\text{sr}$)			Assignment	$S_{\text{EXP}}^{\text{AV}}$	S_{TH}	S_{MIX}	U^2
		60°	60°	90°					
1	0 ± 3	2.0 ± 0.3	1.8 ± 0.6	1.9 ± 0.4	$\frac{3}{2}^+$ [411†]	0.05	0.02	0.02	0.6
2	61 ± 2	73.4 ± 5.4	50.2 ± 4.5	28.7 ± 2.2	$\frac{5}{2}^+$ [411†]	1.0	0.98	1.2	0.6
3	144 ± 3	1.7 ± 0.4	2.1 ± 0.6	2.7 ± 0.4	$\frac{7}{2}^+$ [411†]	0.11	0.14	0.20	0.6
4	252 ± 2	3.2 ± 0.4	2.1 ± 0.6	4.6 ± 0.9	$\frac{3}{2}^+$ [411†]	0.21 ^a	0.06	0.06	0.6
5	326 ± 3	1.4 ± 0.3			$\frac{5}{2}^+$ [413†]	0.02	0.02	0.05	0.4
6	357 ± 3	3.0 ± 0.4	0.7 ± 0.5	1.4 ± 0.3	$\frac{7}{2}^-$ [532†]	0.03	0.02	0.04	0.3
7	408 ± 2	9.5 ± 0.7	20.3 ± 4.2	10.4 ± 0.9	$\frac{7}{2}^+$ [413†]	0.62	0.76	1.7	0.4
8	427 ± 3	0.9 ± 0.3							
9	515 ± 2	23.0 ± 4.7	49.3 ± 3.5	19.1 ± 2.0	$\frac{11}{2}^-$ [532†]	1.5	0.57	2.1	0.3
10	595 ± 5	7.6 ± 1.1	1.7 ± 0.6	0.8 ± 0.3	$\frac{1}{2}^+$ [411†] γ	0.04			
11	633 ± 2	21.3 ± 2.4	15.4 ± 2.1	10.3 ± 1.5	$\frac{3}{2}^+$ [411†] γ	0.35			
12	657 ± 4	30.6 ± 4.4	34.8 ± 3.3	17.9 ± 3.6	$\frac{7}{2}^+$ [404†]	1.3	1.8	1.2	0.9
13	691 ± 4	16.2 ± 1.1	6.4 ± 2.0	6.8 ± 2.4	$\frac{5}{2}^+$ [411†] γ	0.21			
14	710 ± 3		5.3 ± 1.6	2.2 ± 0.6					
15	788 ± 4	4.5 ± 0.5	2.3 ± 0.5	5.2 ± 1.3	$\frac{7}{2}^+$ [411†] γ	0.15			
16	837 ± 3	116.5 ± 7.0	52.8 ± 4.3	42.1 ± 7.9	$\frac{5}{2}^+$ [402†]	1.5	1.9	1.7	1.0
17	889 ± 3	25.0 ± 5.7	3.3 ± 1.6	3.2 ± 1.3					
18	923 ± 3	53.2 ± 2.7	16.0 ± 6.4	11.3 ± 0.9	$\frac{1}{2}^+$, $\frac{3}{2}^+$ [411†]	0.10, 0.44 ^b	0.23, 1.1	0.23, 1.1	1.0
19	965 ± 3	18.6 ± 1.1	3.8 ± 0.9	3.5 ± 0.5	$(\frac{1}{2}^- [541†])$	0.09	0.09		1.0
20	1004 ± 3	18.3 ± 2.2	3.4 ± 0.9	6.3 ± 0.9	$(\frac{5}{2}^- [541†])$	0.17	0.40		1.0
21	1047 ± 3	6.6 ± 0.8	11.5 ± 1.7	2.7 ± 0.7	$\frac{5}{2}^+$ [411†]	0.23	0.37	0.35	1.0
22	1067 ± 4	5.9 ± 1.2	4.4 ± 1.5	4.8 ± 0.8	$\frac{7}{2}^+$ [411†]	0.27	0.26	0.27	1.0
23	1109 ± 3	4.2 ± 1.0							
24	1198 ± 2	4.5 ± 0.6							
25	1455 ± 4	25.8 ± 7.7							
26	1529 ± 3	7.4 ± 1.0							
27	1541 ± 3	35.8 ± 2.9							

^a Peak believed to be a multiplet.

^b Peak believed to be a multiplet; S extracted by dividing experimental strength in ratio of theoretical strengths.

over the small-mass region produced virtually no change in the relative energies of the different levels.

One of the observable effects of the pairing correlations is that the excitation energy of a given state is lowered from the Nilsson prediction, an

effect that is approximated¹⁰ by

$$E_{ij} \approx [(\epsilon_{ij} - \lambda)^2 + \Delta^2]^{1/2} - \Delta, \quad (3)$$

where E_{ij} is the excitation energy, ϵ_{ij} is the Nilsson eigenenergy, λ on the average is the Fermi level, and Δ is one half the pairing gap. The other

TABLE III. ^{159}Tb spectroscopic information. Assignments in parentheses are uncertain.

Line	$E \pm \Delta E$	$\left(\frac{d\sigma}{d\Omega}\right)_{\text{He}, d}$	$\left(\frac{d\sigma}{d\Omega}\right)_{\alpha, t}$		Assignment	$S_{\text{EXP}}^{\text{AV}}$	S_{TH}	S_{MIX}	U^2
		($\mu\text{b}/\text{sr}$)	60°	90°					
1	0±3	1.8±0.4	5.4±0.9	1.5±0.3	$\frac{3}{2}^+$ [411†]	0.05	0.02	0.03	0.6
2	60±2	72.4±6.5	89.4±3.5	38.2±4.2	$\frac{5}{2}^+$ [411†]	1.3	1.0	1.0	0.6
3	138±2	1.5±0.3	2.5±0.9	2.4±0.4	$\frac{7}{2}^+$ [411†]	0.11	0.14	0.19	0.6
4	242±2	4.5±0.5	6.2±0.9	7.0±0.8	$\frac{3}{2}^+$ [411†]	0.31	0.06		0.6
5	386±3	3.2±0.6	2.2±0.6	1.2±0.7	$\frac{7}{2}^-$ [532†]	0.04	0.02	0.04	0.2
6	428±3	6.7±1.5	23.0±1.8	6.2±0.7	$\frac{7}{2}^+$ [413†]	0.46	0.75	0.96	0.4
7	544±2	28.9±5.8	83.1±5.5	23.3±1.6	$\frac{11}{2}^-$ [532†]	2.1	0.87	2.1	0.2
8	580±3	6.5±2.0	1.6±0.8	1.5±0.7	$\frac{1}{2}^+$ [411†] γ	0.05			
9	618±3	27.1±4.6	32.0±2.6	14.7±1.7	$\frac{3}{2}^+$ [411†] γ	0.52			
10	673±3	19.6±4.5	13.1±1.3	8.2±1.2	$\frac{5}{2}^+$ [411†] γ	0.29			
11	777±3	24.1±3.2	54.3±6.3	25.8±3.8	$\frac{7}{2}^+$ [404†]	1.5	1.8	1.6	0.9
12	816±4	6.5±1.0	14.9±1.8	5.3±3.1	($\frac{11}{2}^-$ [523†])	0.43	1.8	0.20	0.9
13	856±3	14.2±5.7	3.7±0.7	5.5±2.1	($\frac{1}{2}^-$ [541†])	0.09	0.10		1.0
14	890±3	21.9±5.9	22.8±3.7	12.8±1.8	($\frac{5}{2}^-$ [541†])	0.47	0.43		1.0
15	944±2	26.9±8.1	5.6±1.0	3.3±0.5					
16	974±3	15.6±3.9	10.9±1.4	5.2±0.6	$\frac{1}{2}^+$, $\frac{3}{2}^+$ [411†]	0.02, 0.17 ^a	0.21, 1.1	0.19, 1.0	1.0
17	1020±4	106.3±21.2	97.4±10.4	59.8±14.1	$\frac{5}{2}^+$ [402†]	1.9	1.9		1.0
18	1045±4	24.3±6.1	8.6±1.7	4.0±0.5					
19	1100±8	11.5±1.8	5.8±1.8	6.9±0.8	$\frac{5}{2}^+$, $\frac{7}{2}^+$ [411†]	0.14, 0.10 ^a	0.38, 0.28	0.32, 0.25	1.0
20	1226±15	2.6±0.5	3.7±1.3	6.0±0.9					
21	1363±3	2.5±0.5							
22	1563±3	3.2±0.5							
23	1638±4	7.0±0.7							
24	1663±3	27.2±2.7							
25	1710±3	6.6±1.4							
26	1743±3	4.1±0.6							
27	1770±3	39.9±5.3							
28	1823±2	6.9±0.7							
29	1872±3	5.9±1.0							
30	1888±3	11.9±1.2							

^a Peak believed to be a multiplet; S extracted by dividing experimental strengths in ratio of theoretical strengths.

TABLE IV. ^{161}Tb spectroscopic information. Assignments in parentheses are uncertain.

Line	$E \pm \Delta E$	$\left(\frac{d\sigma}{d\Omega}\right)_{(\beta\text{He}, d)}$	$\left(\frac{d\sigma}{d\Omega}\right)_{(\alpha, t)}$		Assignment	$S_{\text{EXP}}^{\text{AV}}$	S_{TH}	S_{MIX}	U^2
		$(\mu\text{b}/\text{sr})$ 60°	60°	90°					
1	0±2	1.6±0.3	a	2.4±0.5	$\frac{3}{2}^+[411\uparrow]$	0.07	0.02	0.02	0.6
2	55±2	55.6±4.5	52.0±5.4	34.4±4.6	$\frac{5}{2}^+[411\uparrow]$	1.1	1.0	1.0	0.6
3	130±4	1.8±0.4	4.2±1.1		$\frac{7}{2}^+[411\uparrow]$	0.11	0.14	0.19	0.6
4	230±4	4.8±0.6	10.7±3.0	2.1±0.5	$\frac{3}{2}^+[411\uparrow]$	0.23	0.06		0.6
5	307±6	0.4±0.2			$\frac{5}{2}^+[413\uparrow]$	0.01	0.03	0.05	0.3
6	386±4	1.9±0.6	2.4±1.1	9.4±1.1	$\frac{7}{2}^+[413\uparrow]$	0.22	0.74	0.93	0.3
7	411±6	2.1±0.4	7.4±1.6		$\frac{7}{2}^-[523\uparrow]$	0.06	0.02	0.05	0.9
8	492±10	2.5±0.6	2.7±1.0	2.6±0.6	$(\frac{3}{2}^+[413\uparrow])$	0.13	0.05		0.3
9	552±3	13.7±1.0	7.0±1.4 ^b	8.5±1.0	$(\frac{11}{2}^-[523\uparrow])$	1.0	1.8	2.1	0.9
10	579±4	42.2±3.0	39.0±4.0	34.2±1.6	$(\frac{11}{2}^-[523\uparrow])$	3.2	1.8	2.1	0.9
11	630±4		4.6±1.0						
12	691±3	2.2±0.7	8.5±1.4	3.5±1.0					
13	722±4	1.1±0.3							
14	764±5		3.0±1.0						
15	842±2	1.4±0.3	5.1±1.6		$(\frac{11}{2}^-[532\uparrow])$	0.12	0.38	0.10	0.2
16	914±4	10.0±1.4	4.3±1.0	2.4±0.5					
17	944±4	28.1±1.7	9.9±1.6 ^b	13.4±1.1	$\frac{7}{2}^+[404\uparrow]$	1.3	2.0	1.7	1.0
18	990±5	55.9±7.5	64.8±4.3	33.0±2.4	$\frac{1}{2}^+, \frac{3}{2}^+[411\uparrow]$	0.17, 0.88 ^c	0.21, 1.1	0.21, 1.1	1.0
19	1052±4		7.7±1.3	19.7±1.9	$(\frac{1}{2}^-[541\uparrow])$	0.08 ^c	0.10		1.0
20	1077±4	39.4±4.0	15.0±1.9		$(\frac{3}{2}^-[541\uparrow])$	0.29 ^c	0.44		1.0
21	1101±5	4.4±0.8	5.0±2.2	6.1±1.1	$\frac{5}{2}^+[411\uparrow]$	0.11 ^c	0.38	0.32	1.0
22	1118±3	3.4±1.1	4.8±3.2		$\frac{7}{2}^+[411\uparrow]$	0.14 ^c	0.28	0.27	1.0
23	1133±4	1.7±0.6	6.7±4.6						
24	1165±4	4.3±1.4	3.2±1.8	2.7±2.7	$(\frac{3}{2}^-[541\uparrow])$	0.21	1.1		1.0
25	1204±3			2.2±0.5					
26	1245±5	43.6±2.2	38.4±3.7	17.9±2.4	$\frac{5}{2}^+[402\uparrow]$	0.66	1.3		1.0
27	1285±5	3.8±1.5		3.2±1.0					
28	1344±5	26.3±1.5	21.3±4.6	11.2±1.3					
29	1386±6	1.4±0.5							
30	1405±4	2.7±0.5							
31	1424±2	4.6±0.7	4.6±1.3		$(\frac{7}{2}^-[541\uparrow])$	0.07	0.13		1.0
32	1587±5	8.1±1.4		5.3±1.0					
33	1614±4			5.4±1.3					
34	1717±4	3.6±0.8							
35	1740±3	7.7±1.4							

TABLE IV (Continued)

Line	$E \pm \Delta E$	$\left(\frac{d\sigma}{d\Omega}\right)_{({}^3\text{He}, d)}$ ($\mu\text{b/sr}$)		$\left(\frac{d\sigma}{d\Omega}\right)_{(\alpha, t)}$ ($\mu\text{b/sr}$)		Assignment	$S_{\text{EXP}}^{\text{AV}}$	S_{TH}	S_{MIX}	U^2
		60°	60°	90°						
36	1774 ± 5			5.6 ± 1.9						
37	1805 ± 3	5.0 ± 0.8								
38	1830 ± 4	19.9 ± 4.0								

^a Peak present; too small to be fitted.

^b Not used in calculating average.

^c Peak believed to be a multiplet; S extracted by dividing experimental strength in ratio of theoretical strengths.

observable effect of pairing is the proportionality of the stripping cross section to the emptiness probability, U^2 , as given in Eq. (1). One may write U^2 as

$$U^2 \approx \frac{1}{2} \left[1 + \frac{(\epsilon_{ij} - \lambda)}{[(\epsilon_{ij} - \lambda)^2 + \Delta^2]^{1/2}} \right], \quad (4)$$

and since previous calculations¹¹ for ¹⁵⁵Tb had found

$$\lambda < E_{\text{g.s.}}, \quad (5)$$

we used $U^2 = 0.6$ for the ground-state band as a first estimate. With this estimate, we correlated energy systematics and intensity patterns in our (³He, d) spectra with known states. No attempt was made to obtain absolute DWBA cross sections by using the renormalization factor of Bassel¹² and varying the inner radial cutoff and finite-range parameters, which change the magnitude of the DWBA cross sections. Since the ground-state band is expected to have a well-characterized, intense, $\frac{5}{2}^+$ member, we normalized to the

TABLE V. Optical-model parameters. The potential form used is

$$U(r) = -V(1 + e^X)^{-1} - i \left[W - 4W_a \left(\frac{d}{dX'} \right) \right] (1 + e^{X'})^{-1},$$

where

$$X = (r - r_0 A^{1/3})/a; \text{ similarly for } X'.$$

	V (MeV)	r_0 (fm)	a (fm)	W (MeV)	r'_0 (fm)	a' (fm)	W_a (MeV)	$r_0 C$ (fm)
p	a	1.25	0.65					1.25
d^b	111.0	1.05	0.86	0	1.24	0.79	17.7	1.25
i^c	200.0	1.40	0.60	50.0	1.40	0.60	0	1.25
³ He ^b	175.0	1.14	0.72	17.5	1.60	0.81	0	1.40
⁴ He ^c	200.0	1.40	0.60	20.0	1.40	0.60	0	1.40

^a V determined in bound-state search. Reference 5.

^b Reference 6.

^c Reference 7.

expected, Coriolis-mixed, strength in this transition in the (³He, d) experiments. We achieved an over-all renormalization factor of 8.7 for the (³He, d) experiments in the zero-range approximation, with no inner radial cutoff. Spectroscopic factors extracted by this procedure were used in combination with the DWBA cross sections to obtain an (α, t) renormalization factor of 110.

Better pairing estimates were obtained after several levels of a nucleus had been identified. With the constraint that $U_{\text{g.s.}}^2 \approx 0.6$, λ and Δ were fitted using experimental excitation energies and Nilsson eigenenergies at various ϵ_2 values. The “best-fit” set of parameters λ , Δ , and ϵ_2 were then used to estimate both excitation energies and emptiness probabilities, U^2 , for the Nilsson configurations expected.

The final correction to the theoretical estimate was the inclusion of $\Delta K = 1$ Coriolis interactions. The Coriolis calculation consisted of diagonalization of the rotational energy matrix where the off-diagonal terms connect two states of identical spin and parity, with K and $K' = K + 1$,

$$\begin{aligned} \langle K | H_{\text{Coriolis}} | K + 1 \rangle_I &= [-\hbar^2 / 2\mathcal{G}_0] \sum_j C_{ji}^K C_{ji}^{K'} [(j - K)(j + K + 1)]^{1/2} \\ &\quad \times [(I - K)(I + K + 1)]^{1/2} (U_K U_{K+1} + V_K V_{K+1}), \end{aligned} \quad (6)$$

where V_K is the occupation amplitude of the level with I, K :

$$U_K^2 + V_K^2 = 1. \quad (7)$$

When $K = \frac{1}{2}$ there is an added diagonal term

$$\langle \frac{1}{2} | H_{\text{Coriolis}} | \frac{1}{2} \rangle = (-1)^{I+1/2} (\hbar^2 / 2\mathcal{G}_0) (I + \frac{1}{2}) a, \quad (8)$$

where a , the decoupling parameter, is given by

$$a \equiv \sum_j (-1)^{j+1/2} (j + \frac{1}{2}) |C_{jI}|^2. \quad (9)$$

Bands included in the calculation were those ex-

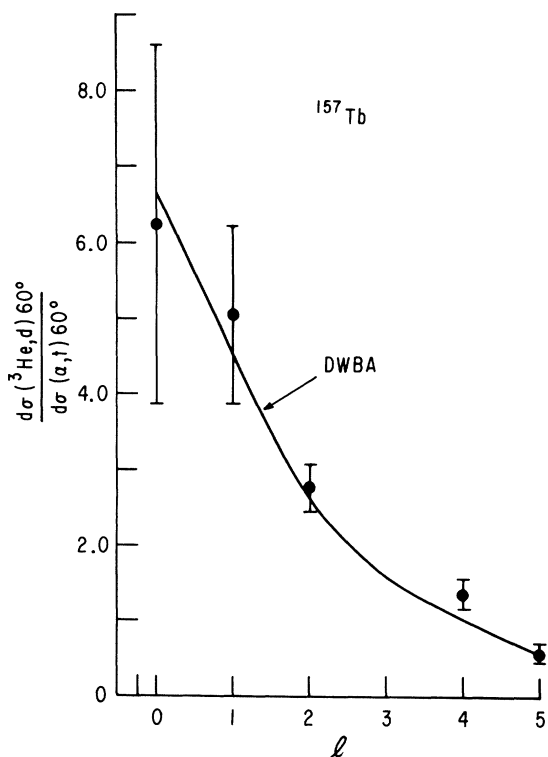


FIG. 3. Angular momentum dependence of the ratio $d\sigma(^3\text{He}, d)/d\sigma(\alpha, t)$ for states excited in ^{157}Tb . Excitation-energy dependence is removed by adjusting all values to $E_{\text{exc}} = 1$ MeV. Points for $l=2, 4$ represent averages of two or more ratios.

pected to be seen in the Tb nuclei, the $[411\uparrow]$, $[411\uparrow]$, $[404\uparrow]$, and either the $[402\uparrow]$ or $[413\uparrow]$ depending on which was more strongly mixed, in the even-parity case, and the $[532\uparrow]$ and $[523\uparrow]$ in the odd-parity case. In ^{155}Tb the $[514\uparrow]$ was included in the latter calculation. In addition to the perturbation of the excitation energies, Coriolis effects also influence the spectroscopic factors, since the mixing amplitudes a_i enter the expression for the spectroscopic factor

$$S_{ij} = 2\left(\sum_i a_i C_{ji}^i U_i\right)^2. \quad (10)$$

Identification of previously unknown states was based on a comparison of excitation energy, rotational energy pattern, and intensity pattern to the theoretical estimates. In addition, the l discrimination afforded by the comparison of the excitation of a given state in the two different experiments yielded meaningful l values for many states. The usefulness of this ratio is seen in Fig. 3, where ratios of states excited in ^{157}Tb are plotted against the DWBA prediction. In $^{157-161}\text{Tb}$, two ratios were available, since the ratio $R' = d\sigma(^3\text{He}, d)/d\sigma(\alpha, t)^{90^\circ}$ also yields usable l information.

IV. DISCUSSION

The assignments in the four nuclei studied are given along with the extracted spectroscopic factors in Tables I-IV. Also given are the theoret-

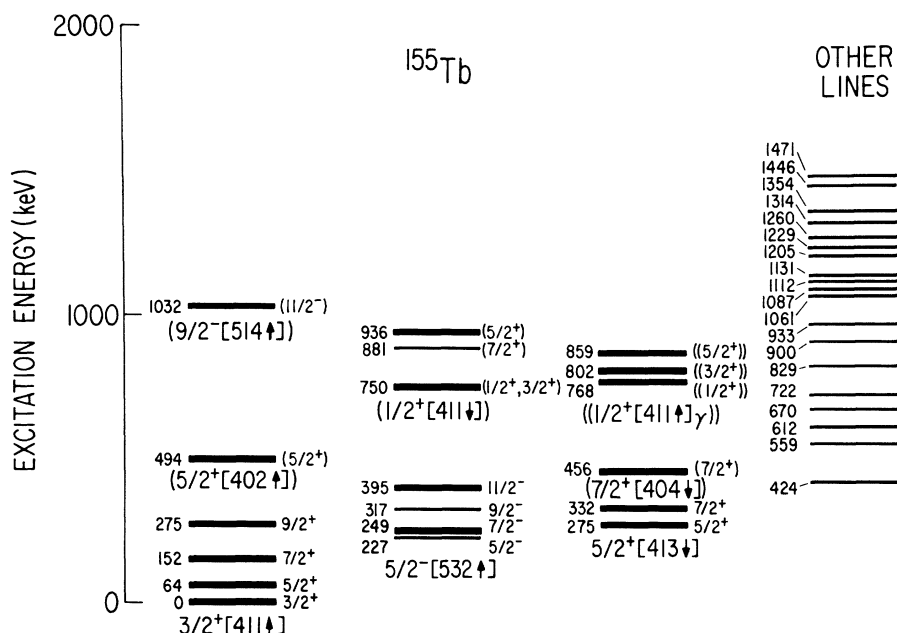


FIG. 4. Level structure of ^{155}Tb . Bands not seen in our experiments are not shown. The thicker lines indicate levels seen in our experiments, while the thinner lines indicate previously identified levels not excited by proton transfer. Parentheses indicate indefinite assignments. The double parentheses indicate a very weak assignment.

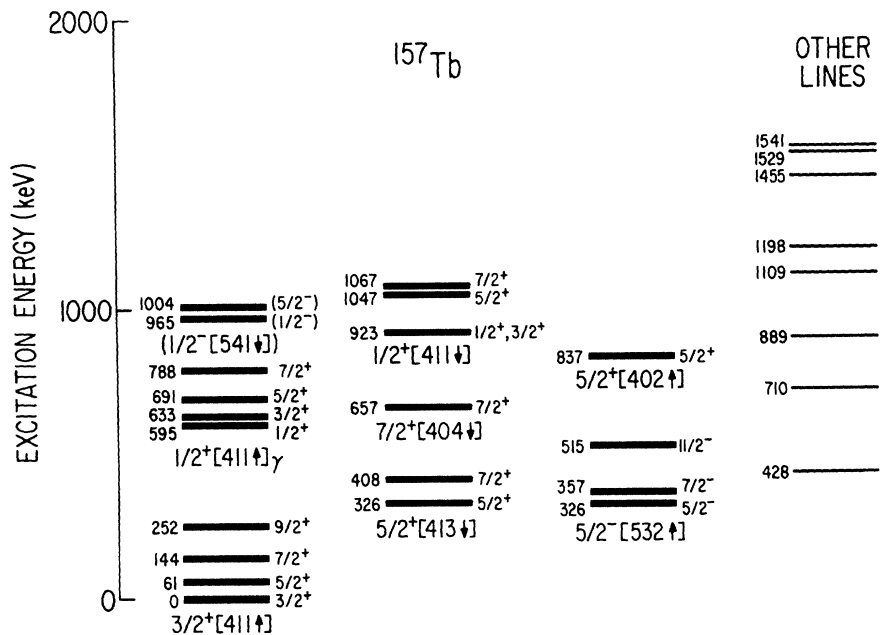


FIG. 5. Level structure of ^{157}Tb . Refer to the caption of Fig. 4 for details of this figure.

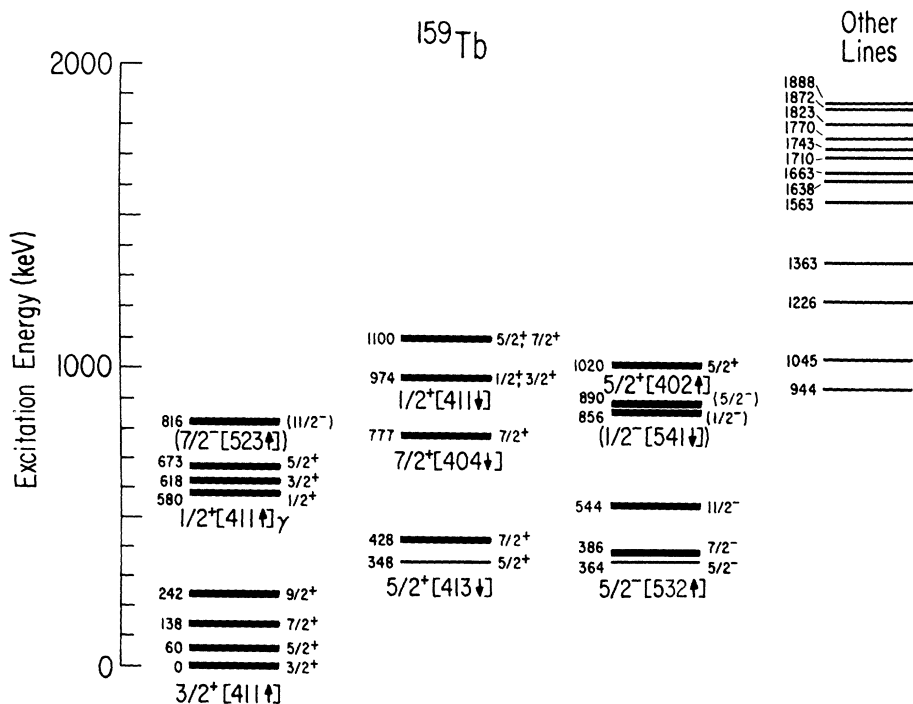


FIG. 6. Level structure of ^{159}Tb . Refer to the caption of Fig. 4 for details of this figure.

ical values of $S = 2C_{ji}^2 U^2$ taken without Coriolis coupling, and the values of $S = 2(\sum_i a_i C_{ji}^2 U_i)^2$ which are the results of our mixing calculations. Level schemes deduced by combining our data with previously known data are depicted in Figs. 4-7. To simplify the discussion of the assignments the configurations identified will be separated by shell-model origin.

A. $d_{5/2}$ States $[411\uparrow]$ and $[402\uparrow]$

In the Tb nuclei studied, the ground-state configuration is the $[411\uparrow]$. It has a well-established spectroscopic pattern, $S_K : S_{K+1} : S_{K+2} : S_{K+3}$, of $0.06 : 1.2 : 0.13 : 0.26$ for the $\frac{3}{2}^+$ through $\frac{9}{2}^+$ members, respectively. This agrees fairly well with the theoretical prediction of $0.02 : 1.2 : 0.22 : 0.06$, which includes Coriolis mixing, although it is relatively unimportant for this band.

The agreement of the $\frac{5}{2}^+$ member over all is due to the renormalization, but there is a remarkable consistency in the results for the different Tb nuclei, an observation which is generally true for the $\frac{3}{2}^+$ and $\frac{7}{2}^+$ members as well. The l values obtained from the ratios agree with these assignments except for the $\frac{7}{2}^+$ state in ^{155}Tb , which is predicted to be $l=3$, and the $\frac{3}{2}^+$ state in ^{161}Tb , where $l=5$ is predicted. It is not unexpected that some l values, extracted for weakly excited states, will be at variance with the level assignment.

The $\frac{9}{2}^+$ member is much more strongly excited than expected. The line is weak on an absolute basis, and the shape was less stable than for other lines, so that, in some cases, it resembled a doublet. Strong Coriolis effects are thought to be a poor explanation of this strength, as the total $\frac{9}{2}^+$ strength in the $d_{5/2}$ bands is less than that seen in just the $[411\uparrow]$ band. It is possible that multi-step processes are significant for this state although our DWBA calculations cannot yield any information on this possibility.

The first-order rotational parameters $A = \hbar^2/2\mathcal{I}_0$ decrease steadily from 13.0 keV in ^{155}Tb to 10.9 keV in ^{161}Tb , which is indicative of the increasing deformation.

The other state with $d_{5/2}$ parentage which we excite in stripping is the $[402\uparrow]$ configuration. The $\frac{5}{2}^+$ member of this band is expected to be strongly excited, and it is a strong line in all our spectra.

The l values extracted from cross-section ratios are all $l=2$ for this state, with the exception of ^{155}Tb , where the $l=3$ extracted causes us to make this an indefinite assignment. The extracted spectroscopic factors agree well with theory except in ^{161}Tb , where the experimental value is only one half the expected value. The higher excitation energy of this state in ^{161}Tb may be the reason for the reduced strength, since states above 1 MeV in excitation are often fractionated in strength. The theoretical values given for ^{159}Tb

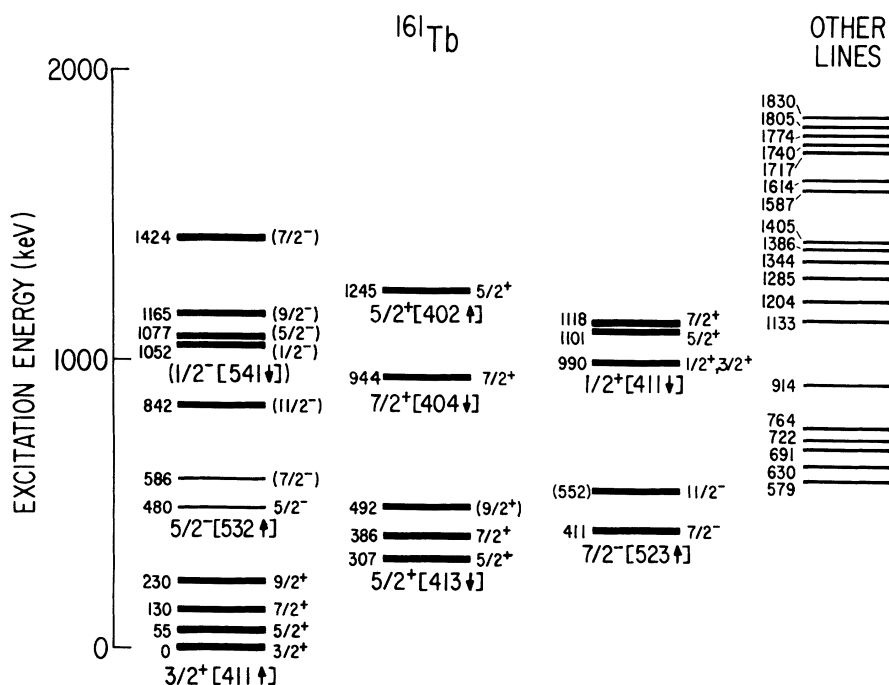


FIG. 7. Level structure of ^{161}Tb . Refer to the caption of Fig. 4 for details of this figure.

and ^{161}Tb are unmixed values, since mixing is expected to be negligible for these states. In ^{155}Tb and ^{157}Tb , the greater proximity of the $[402\uparrow]$ to the $[411\uparrow]$ configuration yields a larger mixing, although agreement in ^{155}Tb is better when the unmixed value is compared. This is perhaps an indication that the unhindered mixing is overestimated in this case.

A systematic comparison of experimental and theoretical band-head energies for these states is given in Fig. 8. No information is obtained about the description of the ground state, since both the experimental and theoretical values have been normalized to 0 keV. The $[402\uparrow]$ configuration appears consistently below the theoretical prediction by 100–300 keV. The discrepancy in energy is, we believe, due to the approximate nature of the pairing calculation. The predicted energy variation with changing deformation is seen to follow closely the experimental value. It appears that at least qualitatively the Nilsson model describes the features of this band, when pairing corrections are included.

B. $d_{3/2}$ State $[411\downarrow]$

This band, which is seen in nuclei with $Z \geq 67$ in good agreement with theory, is expected to be quite difficult to describe in the Tb nuclei. Bes and Cho¹³ and Soloviev and Fedotov¹⁴ both predict two $K^\pi = \frac{1}{2}^+$ bands, the first being about 50% single particle and having a decoupling parameter a near that expected for the $[411\uparrow]$ configuration. The state is expected to be fairly low in excitation, at

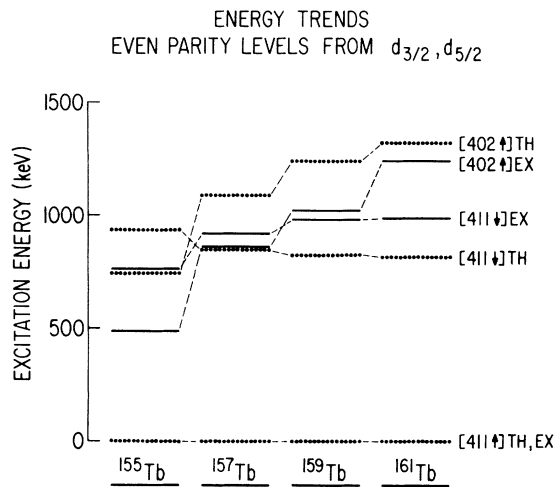


FIG. 8. A comparison of experimental and theoretical band-head energies for states in the Tb nuclei which come from the $d_{3/2}$ and $d_{5/2}$ shell-model states. The theoretical prediction includes pairing effects, but not Coriolis-coupling effects.

about 500 keV. The second $K^\pi = \frac{1}{2}^+$ state is expected at 1000 keV, and is expected to have virtually no single-particle character. The reason for the fractionation of strength is mixing with γ vibrations of which there can be two with $K^\pi = \frac{1}{2}^+$, a $[411\uparrow]\gamma$ and a $[413\uparrow]\gamma$.

Our experimental evidence does yield two $K^\pi = \frac{1}{2}^+$ bands, although their character is not well described by the Nilsson model or by the superfluid calculations of Refs. 13 and 14. The evidence in ^{155}Tb is considered weaker than in the other nuclei, and it will be considered separately.

We have identified in $^{157, 159, 161}\text{Tb}$ the $[411\uparrow]$ single-particle band at 923, 974, and 990 keV, respectively. The energy systematics are quite straightforward. In ^{159}Tb , Diamond, Elbek, and Stephens¹⁵ tentatively describe this band at 971, 979, 1087, and 1103 keV for the $\frac{1}{2}^+$, $\frac{3}{2}^+$, $\frac{5}{2}^+$, and $\frac{7}{2}^+$ members, yielding a decoupling parameter $a = -0.81$. In ^{157}Tb , our fit of the $\frac{1}{2}^+$, $\frac{3}{2}^+$ doublet at 923 keV, $\frac{5}{2}^+$ at 1047 keV, and $\frac{7}{2}^+$ at 1067 keV yields $A = 10.4$ keV, $a = -0.79$; in ^{159}Tb we have two doublets, the $\frac{1}{2}^+$, $\frac{3}{2}^+$ at 974 keV, and the $\frac{5}{2}^+$, $\frac{7}{2}^+$ at 1100 keV, yielding $A \approx 12.6$ keV, $a \approx -0.80$. In ^{161}Tb where the energies are $\frac{1}{2}^+$, $\frac{3}{2}^+$ at 990 keV, $\frac{5}{2}^+$ at 1101 keV, and $\frac{7}{2}^+$ at 1118 keV, we obtain $A = 12.4$ keV, $a = -0.81$. These rotational fits yield decoupling parameters very close to the theoretical value of $a = -0.80$.

Although no ratios were calculated for the doublets, which are of mixed l , those singlet ratios which were available did yield values consistent with the assignments.

Identification of these configurations by intensity pattern is quite difficult, but a cogent explanation of the situation may be obtained by looking at the lower $K^\pi = \frac{1}{2}^+$ bands in ^{157}Tb and ^{159}Tb .

We make assignment of $K^\pi = \frac{1}{2}^+$ bands in ^{157}Tb and ^{159}Tb , which we identify as γ vibrations with significant single-particle strength. Since the predominant vibrational character is believed to be based on the ground-state band, we use the notation $[411\uparrow]\gamma$. In ^{157}Tb this band has been identified through a (p, t) study.¹⁶ This band has also been identified in ^{159}Tb .¹⁷ The bands in these two nuclei are quite similar, having intensity ratios roughly 1:10:6, with slight, positive decoupling parameters $a = +0.07$ and $a = +0.09$, respectively.

The l values extracted for these states are in agreement with the assignments with strong $l=0$ identification for the $\frac{1}{2}^+$ member.

In ^{161}Tb , where no lower $K^\pi = \frac{1}{2}^+$ band has been identified, the $\frac{1}{2}^+$, $\frac{3}{2}^+$ doublet of the $[411\uparrow]$ configuration is populated with 80% of the expected theoretical strength. In ^{157}Tb and ^{159}Tb , the $\frac{1}{2}^+$ and $\frac{3}{2}^+$ strengths are split between the two bands. In ^{157}Tb , about 30% of the theoretical strength is in the lower band, while 40% is in the upper band.

In ^{159}Tb approximately 50% of the $\frac{1}{2}^+$, $\frac{3}{2}^+$ strength is in the lower band, while 40% is in the upper band. The total $\frac{1}{2}^+$, $\frac{3}{2}^+$ strength is similar in all three cases. This effect lends added credence to the contention that the two bands are strongly mixed.

The intensity situation is not easily explained for the $\frac{5}{2}^+$ and $\frac{7}{2}^+$ members, however. In ^{161}Tb , a significant amount of strength is missing from these states in the $[411\downarrow]$ configuration. This is similar in ^{159}Tb , but in this case addition of the $\frac{5}{2}^+$ strength from the γ band brings the total $\frac{5}{2}^+$ strength to a value greater than expected. In ^{157}Tb , where the $\frac{7}{2}^+$ member of the γ configuration is identified, the total strength in both the $\frac{5}{2}^+$ and $\frac{7}{2}^+$ members is greater than the estimate. We have no explanation for this phenomenon, although the superfluid model prediction that the γ band includes some $[413\downarrow]\gamma$ character may be important. This mixing could affect the $\frac{5}{2}^+$ and $\frac{7}{2}^+$ strength.

In ^{155}Tb , the assignments are considered only possible and are more tentative than the probable assignments in the other nuclei. Our assignments of the $\frac{1}{2}^+$, $\frac{3}{2}^+$ doublet and the $\frac{5}{2}^+$ state of the $[411\downarrow]$ single-particle configuration agree with those of Mihelich and Harmatz,¹⁸ and yield a decoupling parameter $a \approx -1.5$, in fair agreement with the theoretical value. The missing $\frac{7}{2}^+$ state is expected to be weak, and its absence is not considered a drawback to the assignment. The missing strength argument, however, demands a γ band with single-particle strength for the other states, and only weak evidence for this configuration is available. States which fit a recognizable rotational pattern are excited at 768, 802, and 859 keV, for the $\frac{1}{2}^+$, $\frac{3}{2}^+$, and $\frac{5}{2}^+$ members, but the spectroscopic ratios in this band, 1:4:4, do not correspond to the ratios obtained in ^{157}Tb and ^{159}Tb for the $[411\downarrow]\gamma$ configuration.

The single-particle configuration is also found to be in poor agreement with the Nilsson-plus-pairing prediction, as can be seen in Fig. 8. Energy shifts due to Coriolis mixing are expected to be small, but the effects of the other coupling on the energy systematics are largely unknown. It is clear, however, that the Nilsson-plus-pairing model fails in this case.

C. $g_{7/2}$ States $[413\downarrow]$ and $[404\downarrow]$

The $[413\downarrow]$ configuration, which is expected to be a hole state, is well known in these Tb nuclei, having been identified in all of those studied save ^{157}Tb .³ The characterization of the members of this band varies over the series of isotopes, an effect which is only partially explained by the change in Coriolis coupling with the $[404\downarrow]$ band,

which varies sharply in energy over this series.

As expected from the theoretical estimate, the $\frac{5}{2}^+$ member of this band is quite weakly excited. In ^{159}Tb it is not measurably excited in our experiments. No l values from ratios are available, although previous identification of this line allows us to make probable assignments.

Identification of the $\frac{7}{2}^+$ member is equally straightforward, since this state as well has been identified previously in $^{155}, ^{159}, ^{161}\text{Tb}$. The l values extracted from these lines agree with the assignments except in ^{161}Tb where $l=2$ is indicated.

Rotational parameters and spectroscopic factors extracted vary somewhat as one goes from ^{155}Tb to ^{161}Tb , which suggests that the unhindered coupling to the $[404\downarrow]$ is important. The $\frac{7}{2}^+$ member of the latter configuration is identified here in all the nuclei studied, albeit tentatively in ^{155}Tb , at 456, 657, 777, and 944 keV in $^{155-161}\text{Tb}$, respectively. The change in energy is expected to have some effect on the relative intensity of the $\frac{7}{2}^+$ members as the Coriolis effects change.

It appears, however, that two situations are present. In $^{157-161}\text{Tb}$, the coupling appears relatively stable. The spectroscopic factors for the $\frac{1}{2}^+[413\downarrow]$ are $S=0.62, 0.46, \text{ and } 0.22$, respectively, indicating some shift in intensity. The S factors for the $\frac{7}{2}^+[404\downarrow]$ are $S=1.3, 1.5, 1.3$, respectively, showing no recognizable change. The rotational parameters for the $[413\downarrow]$ band are in accord with the premise that the coupling changes only slightly, $A \approx 11.7, 11.4, \text{ and } 11.3$ keV, respectively, in $^{157-161}\text{Tb}$. Our mixing calculation does not predict this situation, even yielding the wrong direction for the intensity shift.

The second case is in ^{155}Tb , where the mixing calculation works fairly well. In this case, $A_{[413\downarrow]} \approx 8.1$ keV, indicative of a strong mixing, and $S_{7/2^+[413\downarrow]}=1.3$, with $S_{7/2^+[404\downarrow]}=0.48$. The calculation overestimates the mixing in this case, but the qualitative prediction is good.

The fact that the total spectroscopic strength, $2C_{jt}^2$, in the two $\frac{7}{2}^+$ states decreases steadily from ^{155}Tb to ^{161}Tb may be indicative of a coupling situation which we have not included. This could be coupling with other bands, higher in energy, that are not identified, and which are not in the coupling calculation. In addition to these states, the $\frac{9}{2}^+[413\downarrow]$ state is tentatively identified in ^{161}Tb in fair agreement with theory.

Figure 9 shows the good agreement of the Nilsson-plus-pairing prediction when compared to the experimental band-head energies of the $[404\downarrow]$. The larger discrepancy in ^{155}Tb is believed to be due to the Coriolis coupling, where the $\frac{7}{2}^+[404\downarrow]$ state is "pushed away" from the $\frac{7}{2}^+[413\downarrow]$. The

[413 \uparrow] is in reasonable agreement with theory, although for bands this close to the ground state, the approximate nature of the pairing calculation limits any expectation of absolute agreement.

D. $h_{11/2}$ States [532 \uparrow], [523 \uparrow], and [514 \uparrow]

The [532 \uparrow] and [523 \uparrow] configurations are expected to be so strongly coupled in the Tb nuclei that identification of an odd-parity state as belonging solely to one band or the other is impossible. Of the two states of spin I , the one which has the lower energy is enhanced. One expects to excite $\frac{7}{2}^-$ and $\frac{11}{2}^-$ states which contain virtually all the single-particle strength expected for that spin value in both bands. We believe the enhanced $\frac{7}{2}^-$ and $\frac{11}{2}^-$ states are based on the [532 \uparrow] configuration in $^{155-159}\text{Tb}$, and on the [523 \uparrow] configuration in ^{161}Tb . These somewhat artificial judgments are based on the position of the $\frac{5}{2}^-$ member of the [532 \uparrow] in most cases. Once this is known, a study of the plausibility of the rotational parameter obtained by assuming the $\frac{7}{2}^-$ and $\frac{11}{2}^-$ to be the [532 \uparrow] or [523 \uparrow] configuration yields a reasonable idea of the base state. In ^{161}Tb , there is an allowed unhindered transition from ^{161}Gd , which has a [523 \uparrow] ground state, to the $\frac{7}{2}^-$ at 417 keV,¹⁹ which gives excellent credibility to the [523 \uparrow] assignment.

The enhanced $\frac{7}{2}^-$ states are seen in good agreement with the theoretical prediction considering the weakness of the excitation.

In general, the enhanced $\frac{11}{2}^-$ states agree quite well with the mixed theory estimates. The improvement is noticeable in $^{155, 157, 159}\text{Tb}$, where the unmixed spectroscopic factor is quite low. In ^{155}Tb , the inclusion of the tentatively identified $\frac{11}{2}^-$ [514 \uparrow] state at 1032 keV is an important part

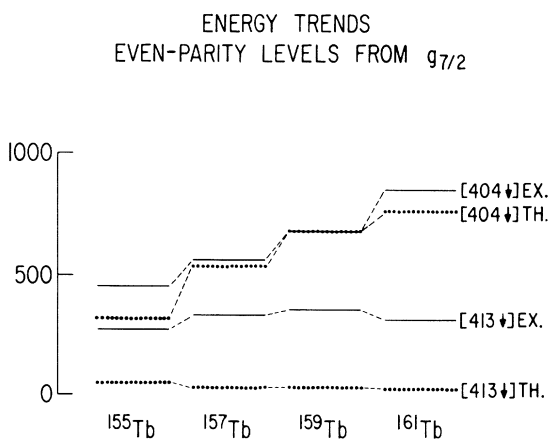


FIG. 9. A comparison of experimental and theoretical band-head energies for states in the Tb nuclei which come from the $g_{7/2}$ shell-model state.

of the mixing calculation. Strong indications of $l=5$ are obtained from the cross-section ratios in $^{155, 157, 159}\text{Tb}$.

In ^{161}Tb , the assignment of the $\frac{11}{2}^-$ is not as clear as in the lighter nuclei. There are two lines, neither of which is well characterized, which yield good rotational parameters when taken in conjunction with the well-established $\frac{7}{2}^-$ assignment. The line at 552 keV yields spectroscopic factors which are smaller than theory, while the 579-keV line yields spectroscopic factors which average 50% greater than theory. The tentative assignment here is made for both energies, since one of these lines is almost certainly the $\frac{11}{2}^-$ [523 \uparrow]. The l values extracted are $l=3 \pm 1$ in either case.

In ^{159}Tb and ^{161}Tb , the depleted $\frac{11}{2}^-$ are assigned tentatively at 816 and 842 keV, respectively. The mixing calculation predicts this state to be in the 800-keV region, and the extracted spectroscopic factors are in reasonable agreement with the prediction. The l values of both are $l=5$ from the cross-section ratios.

The $\frac{11}{2}^-$ state of the [514 \uparrow] configuration is tentatively identified in ^{155}Tb . The energy fits reasonably with that predicted in the mixing calculation, the l estimated is $l=5$, and the spectroscopic factor extracted is in reasonable agreement with theory.

The agreement of the theoretical and experimental band-head energies is given in Fig. 10. The predicted variation of energy is quite good for the [532 \uparrow] configuration.

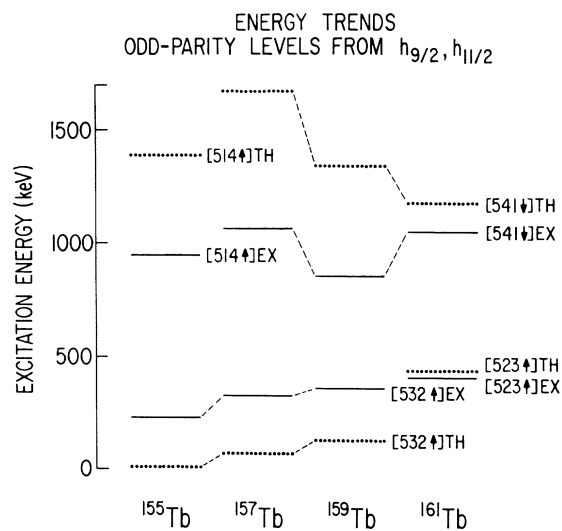


FIG. 10. Comparison of theory and experiment for the excitation energies of states in the Tb nuclei. The configurations shown here derive from the $h_{9/2}$ and $h_{11/2}$ shell-model states.

E. $h_{9/2}$ Level [541↓]

This band has a large positive decoupling parameter $a \approx 4$ and can be so strongly coupled to the [532↓] configuration, as to eliminate the typical rotational pattern. Our tentative assignments of the $\frac{1}{2}^-$, $\frac{5}{2}^-$ in $^{157,159}\text{Tb}$ and the $\frac{1}{2}^-$, $\frac{5}{2}^-$, $\frac{7}{2}^-$, and $\frac{9}{2}^-$ in ^{161}Tb are consistent with a large decoupling parameter.

The $\frac{1}{2}^-$ and $\frac{5}{2}^-$ assignments are in reasonable agreement with theory when the energy and intensity systematics are considered. In addition the l values from the ratios are correct in ^{157}Tb and ^{159}Tb , with the ^{161}Tb ratios being obscured by the doublet.

The poor agreement of the extracted S factors for the $\frac{7}{2}^-$ and $\frac{9}{2}^-$ lines in ^{161}Tb , and the absence

of identifiable $\frac{7}{2}^-$ and $\frac{9}{2}^-$ states in ^{157}Tb and ^{159}Tb force these assignments into the tentative category.

ACKNOWLEDGMENTS

The authors would like to thank Thomas Elze for his assistance in these experiments, and W. P. Alford for his valuable comments. We are grateful to J. Lerner of the Argonne National Laboratory for making the targets on the ANL isotope separator. Thanks are also due the support staff of the Nuclear Structure Research Laboratory, especially the accelerator operators for their cooperation, George Korn for his plate development, and Mrs. A. Izaks for her careful plate scanning. The support of the Nuclear Structure Research Laboratory by the National Science Foundation is gratefully acknowledged.

*Work supported by the U. S. Atomic Energy Commission.

†Work supported by a DuPont Science and Technology Grant, 1970–1972.

¹G. R. Satchler, *Ann. Phys. (N.Y.)* **3**, 275 (1958).

²Th. W. Elze and J. R. Huizenga, *Nucl. Phys. A149*, 585 (1970); *Phys. Rev. C* **1**, 328 (1970).

³M. E. Bunker and C. W. Reich, *Rev. Mod. Phys.* **43**, 348 (1971).

⁴We are indebted to J. Lerner of Argonne National Laboratory for making these targets on the ANL isotope separator.

⁵R. H. Bassel, R. M. Drisko, and G. R. Satchler, Oak Ridge National Laboratory Report No. ORNL-3240, 1962 (unpublished).

⁶B. H. Wildenthal, B. M. Preedom, E. Newman, and M. R. Cates, *Phys. Rev. Letters* **19**, 960 (1967).

⁷J. S. Lilley and N. Stein, *Phys. Rev. Letters* **19**, 109 (1967); **19**, 1000 (1967).

⁸M. T. Lu and W. P. Alford, *Phys. Rev. C* **3**, 1243 (1971).

⁹S. G. Nilsson, C. F. Tsang, A. Sobiczewski, Z. Szymanski, S. Wycech, C. Gustafson, I. L. Lamm, P. Möller, and B. Nilsson, *Nucl. Phys. A131*, 1 (1969).

¹⁰W. Ogle, S. Wahlborn, R. Piepenbring, and S. Frediksson, *Rev. Mod. Phys.* **43**, 424 (1971).

¹¹G. Winter, L. Funke, K. H. Kaun, P. Kemnitz, and H. Sodan, *Phys. Letters* **32B**, 161 (1970).

¹²R. H. Bassel, *Phys. Rev.* **149**, 791 (1966).

¹³D. R. Bes and Y.-C. Cho, *Nucl. Phys.* **86**, 581 (1966).

¹⁴V. G. Soloviev, S. I. Fedotov, Joint Institute for Nuclear Research Report No. E4-6055, 1971 (unpublished).

¹⁵R. M. Diamond, B. Elbek, and F. S. Stephens, *Nucl. Phys.* **43**, 560 (1963).

¹⁶R. W. Goles, R. A. Warner, Wm. C. McHarris, and W. H. Kelly, *Bull. Am. Phys. Soc.* **16**, 1162 (1971).

¹⁷J. C. Hill and M. L. Wiedenbeck, *Nucl. Phys. A111*, 457 (1968).

¹⁸J. W. Mihelich and B. Harnatz, private communication.

¹⁹J. Zylicz, P. G. Hansen, H. L. Nielson, and K. Wilsky, *Nucl. Phys.* **84**, 13 (1966).